

$Pb_2Sr_2(Y_{1-x}Ca_x)Cu_3O_{8+\delta}$ 초전도체 ($x=0.4-0.6$)의 제조방법 및 상평형

최영일·정동운
원광대학교 화학과

Phase Equilibria and Processing of $Pb_2Sr_2(Y_{1-x}Ca_x)Cu_3O_{8+\delta}$ Superconductors
($x = 0.4 - 0.6$)

Young-il Choi and Dongwoon Jung
Department of Chemistry
Wonkwang University
Iksan, Chon-Buk, Korea, 570-749

초 록 $x=0.4-0.6$ 이고 작은 δ 값을 갖는 $Pb_2Sr_2(Y_{1-x}Ca_x)Cu_3O_{8+\delta}$ 초전도체 시료를 제조하였다. 시료가 초전도체로 되기 위하여 작은 δ 값을 가져야 하는데 이를 위해 소결 후 직접 낮은 산소분압에서 annealing하면 산화성 상분해가 발생하여 과잉의 2차상이 생성된다. 따라서 제조과정중 산화성 상분해의 양을 줄이기 위하여 두 단계의 annealing 과정을 도입하였다. 즉 100% 아르곤 기체 분위기에서의 소결 후 먼저 100% 산소 분위기하에서 시료를 annealing하여 산화시킨 후 0.1~1.0% 산소분압하에서 annealing하여 작은 δ 값을 얻는 것이다. 얻어진 시료의 전기저항 측정결과 80K의 초전도 전이온도(T_c)가 얻어져 지금까지 이 화합물에서 보고된 결과중 가장 높은 T_c 를 나타내었다. 그러나 본 연구에서 도입한 두단계 annealing 과정에 의해서도 작은 δ 값을 얻기 위하여는 약간의 산화성 상분해가 발생하여 깨끗한 초전도 전이과정을 볼 수 없었다.

Abstract $Pb_2Sr_2(Y_{1-x}Ca_x)Cu_3O_{8+\delta}$ samples were prepared with $x=0.4\sim 0.6$ and small δ . To minimize the extent of oxidative decomposition reaction which occurs during the preparation of this phase, two annealing steps were adopted: First, sintered samples of $Pb_2Sr_2(Y_{1-x}Ca_x)Cu_3O_{8+\delta}$ are oxygenated under 100% O_2 , which leads to a large δ (e.g., $\delta=1.8$). Second, the resulting samples are deoxygenated under 0.1~1.0% O_2 in N_2 , lowering δ to desired values. This two-step annealing procedure minimized the extent of oxidative decomposition. However, even with the two-step annealing procedure, the oxidative decomposition of $Pb_2Sr_2(Y_{1-x}Ca_x)Cu_3O_{8+\delta}$ cannot be completely suppressed if δ is to be reduced to maximize T_c .

Electrical resistivity data show that $T_c(\text{onset})$ is a function of hole concentration in the CuO_2 layer, and the optimum hole concentration for the maximum T_c is achieved when Ca^{2+} is substituted for Y^{3+} between 0.5 and 0.6. A $T_c(\text{onset})=80K$ has been observed for one such sample, and this is the highest $T_c(\text{onset})$ yet reported for this compound.

I. Introduction

In 1988, Cava et. al.,¹⁾ reported a new family of copper-oxide superconductors with the general formula $Pb_2Sr_2(Y_{1-x}Ca_x)Cu_3O_{8+\delta}$, which hereafter will be referred to as the 2213-phase. This 2213-phase is similar in structure to the Tl- and Bi- families of superconductors

in that it contains the perovskite CuO_2 layers and rock salt Pb-O layers²⁾, but it is unique in that the Pb-O layers are linked by copper atoms [see Fig. 1]. For convenience, we denote the copper of the CuO_2 layers by Cu(1), and that sandwiched between the Pb-O layers by Cu(2)

Copper-oxide superconductors are usually

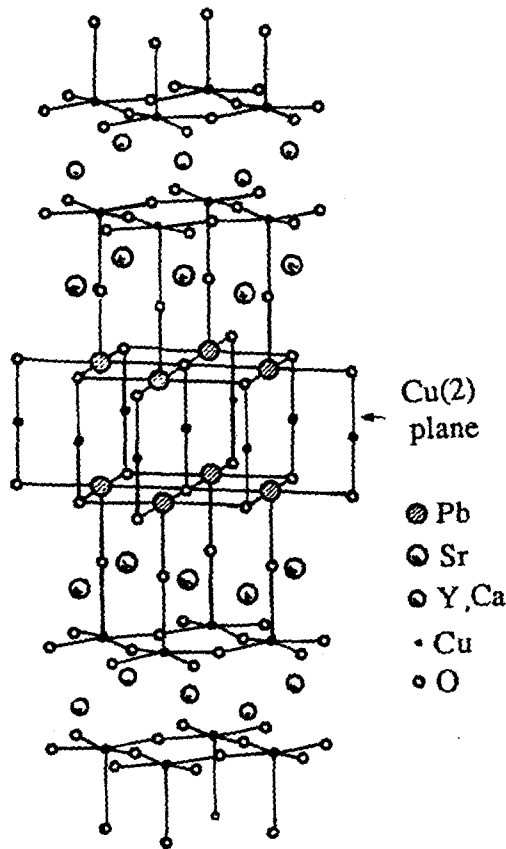


Fig. 1. Schematic representation of the crystal structure of $\text{Pb}_2\text{Sr}_2(\text{Y}_{1-x}\text{Ca}_x)\text{Cu}_3\text{O}_8$.

derived from insulator parent compounds where in copper in the CuO_2 layers is divalent.^{3, 4)} Note that the parent compound for the 2213-phase is $\text{Pb}_2\text{Sr}_2\text{YCu}_3\text{O}_8$, an insulator.⁵⁾ In the parent compound, there is no oxygen in the Cu(2) plane and the formal oxidation state of Cu(1) and Cu(2) are +2 and +1, respectively. The increase of the oxidation state of copper leads to the hole generation in the CuO_2 layer and the resultant compound becomes a p-type superconductor. The T_c of a p-type cuprate superconductor is dependent upon the hole concentration (n_H) in the CuO_2 layer, with a maximum T_c at an optimum n_H value (n_{opt}).⁶⁾ Hole concentration is usually adjusted through cation substitutions (e.g., Sr^{2+} for La^{3+} in La_2CuO_4), variable oxygen stoichiometries (e.g., δ in $\text{YBa}_2\text{Cu}_3\text{O}_{7-\delta}$),

or a combination of both.

In the $\text{Pb}_2\text{Sr}_2(\text{Y}_{1-x}\text{Ca}_x)\text{Cu}_3\text{O}_{8+\delta}$ system, hole generation in the CuO_2 layers is determined primarily by the Ca content (i.e., x value). As Ca^{2+} is substitute for Y^{3+} , the average oxidation state of copper is increased and the T_c of the resulting 2213-phase becomes higher. Cava et.al.⁷⁾ and Subramanian et.al.⁴⁾ have reported that the T_c of the 2213-phase increases with increasing x and the upper limit of the Ca^{2+} substitution is approximately $x=0.5$, and the maximum T_c 's (onset) of their samples are ~ 68 K and ~ 76 K, respectively. Oxygen surplus is another way to increase the oxidation state of copper. As δ increases, oxygen atoms are intercalated into the Cu(2) plane to form Cu(2)-O chains.

However, it has been recognized that in the case of increased Ca substitution (i.e., higher x), oxygen intercalation competes against an oxidative decomposition, thereby resulting in the formation of a nonsuperconducting second phase, which is related to SrPbO_3 .⁷⁾ The oxidative decomposition becomes a more dominant factor as the Ca content is increased or processing temperatures are raised.

In order to understand the dependence of T_c on hole concentration in the $\text{Pb}_2\text{Sr}_2(\text{Y}_{1-x}\text{Ca}_x)\text{Cu}_3\text{O}_{8+\delta}$ system, two goals were pursued: first, a synthetic method was sought which would minimize the oxidative decomposition while controlling the hole concentration. Second, compositions and electronic properties of the resulting samples were determined. In this paper the optimum process for minimizing oxidative decomposition is described, and the dependence of T_c upon the Ca content in the range $x=0.4-0.6$ is examined.

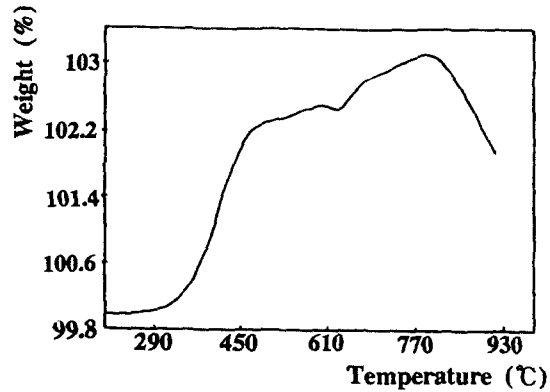
II. Experimental

Stoichiometric amounts of the oxides (Porchem SrO 99.99% CaO99.99% ; Johnson Matthey CuO 99.99% ; Rhone-Poulenc Y_2O_3 99.99%) were thoroughly mixed using a mortar and pestle and pelletized in a 0.5" die under

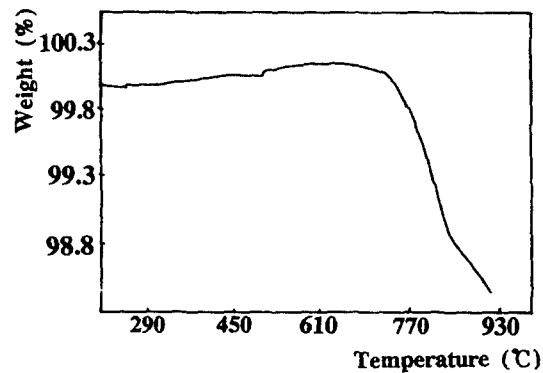
172 MPa (2500 psi) isostatic pressure. Pellets were calcined in a Lindberg muffle furnace in 99.8% dense Al_2O_3 crucibles in air for 16 hours at 920°C with several intermediate grindings. PbO (Prochem 99.99%) was then reacted with the ground pre-reacted precursors in pellet form at $800-920^\circ\text{C}$ for 1-4 hours in 100% Ar (the reaction step). The resulting samples were sintered at $800-920^\circ\text{C}$ for 1-4 hours in 100% Ar (the sintering step.) The sintered samples were annealed at $425-490^\circ\text{C}$ in 100% O_2 gas stream (the oxygenation step). Finally the fully oxygenated samples were annealed under low oxygen pressure (i.e., $0\% < p\text{O}_2 < 1.0\%$) (the deoxygenation step). After each step, samples were examined by powder X-ray diffraction (XRD) using Norelco and Rigaku diffractometers with $\text{Cu K}\alpha$ radiation. Mass changes were monitored throughout the process. To investigate the isothermal mass change as a function of time, thermogravimetric analysis (TGA) were done using a Perkin-Elmer TGA7. A standard dc four-point probe was used for the electrical resistivity measurement in the region from room temperature to 10 K (with cooling rate of $1.6^\circ\text{C}/\text{min}$).

III. Results and Discussions

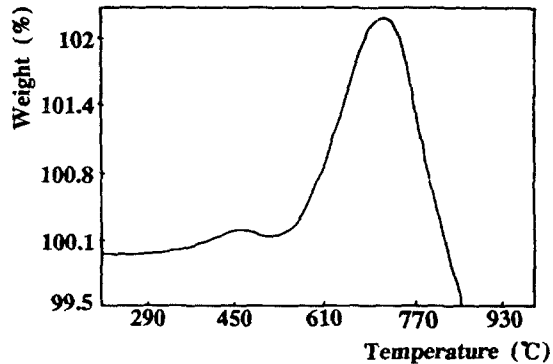
Thermogravimetric analysis curves for $\text{Pb}_2\text{Sr}_2(\text{Y}_{1-x}\text{Ca}_x)\text{Cu}_3\text{O}_{6+\delta}$ are shown in Fig. 2. Fig. 2a shows the TGA plot of $\text{Pb}_2\text{Sr}_2\text{Y}_{0.5}\text{Ca}_{0.5}\text{Cu}_3\text{O}_{6+\delta}$ synthesized in 100% Ar, and run in flowing O_2 . The mass increase occurs in two temperature regimes, which corresponds to two processes. In the range $290-650^\circ\text{C}$, the mass increase corresponds to oxygen intercalation into the $\text{Cu}(2)$ plane. Above 650°C , sample mass increases as a result of the oxidative decomposition. The temperature borderline between intercalation and the decomposition processes decreases with increasing Ca-content (i. e. the decomposition is shifted to lower temperatures). Thus, as shown in Fig. 2a, there is considerable overlap of the two processes. Direct competition between these processes there



(a)



(b)



(c)

Fig. 2. Thermogravimetric analysis curves for $\text{Pb}_2\text{Sr}_2(\text{Y}_{0.5}\text{Ca}_{0.5})\text{Cu}_3\text{O}_{6+\delta}$ synthesized in 100% Ar, and run in flowing (a) 100% O_2 , (b) 0.1% O_2 in N_2 , and (c) 1.0% O_2 in N_2 .

fore impedes synthesis of samples with $x \geq 0.5$. In addition, samples with increased Ca-content show decomposition occurring at lower oxygen partial pressures. This point can be illustrated by

the TGA data shown in Figs. 2b and 2c^{1, 4)}. The weight change of samples of $\text{Pb}_2\text{Sr}_2\text{Y}_{0.5}\text{Ca}_{0.5}\text{Cu}_3\text{O}_{8+\delta}$ reacted and sintered in 100% Ar, are analyzed in the TGA in a flowing gas atmosphere, using 0.1% (see Fig. 2b) and 1% (see Fig. 2c) O_2 , in N_2 . It can be seen that very little mass change occurs in 0.1% O_2 . In contrast, 1% O_2 results in a significant mass increase. The small maximum at $\sim 480^\circ\text{C}$ corresponds to oxygen intercalation. However, the mass change is dominated by the oxidative decomposition which peaks at $\sim 750^\circ\text{C}$. The mass loss at $> 800^\circ\text{C}$ is attributed to PbO evaporation.

A series of experiments were performed in order to determine whether $\text{Pb}_2\text{Sr}_2\text{Y}_{0.5}\text{Ca}_{0.5}\text{Cu}_3\text{O}_{8+\delta}$ could be reacted and sintered in Ar, cooled to room temperature, and then annealed at temperatures lower than 500°C in controlled atmospheres to tune the oxygen content without oxidative decomposition. In our study, the δ values of the 2213-phases are estimated as follows: First we assume that δ after the reaction or sintering step is zero since these two steps are carried out under 100% Ar and the resultant product is $\text{Pb}_2\text{Sr}_2(\text{Y}_{1-x}\text{Ca}_x)\text{Cu}_3\text{O}_8$. Because of the low annealing temperature (i.e., 480°C), the weight changes after the oxygenation and deoxygenation steps are assumed to represent the changes of the oxygen content in the samples. Consequently, δ values are calculated from the weight changes in the oxygenation and the deoxygenation steps. In XRD pattern the major peak at $2\theta = 32.7^\circ$ in each diffraction pattern represents the (114) reflection of the 2213-phase. The two split peaks at $2\theta = 33.3^\circ$ and 33.8° represent the (020) and (200) reflections of the 2213-phase, respectively. In an orthorhombic phase, the d-spacings and peak intensities of the (020) and (200) reflections are different so that the two split peaks appear, while only one peak appears in the tetragonal phase. The samples reacted and sintered in 100% Ar show no oxidative decomposition as shown in Fig. 3a, but a superconducting transition is not observed. Annealing for

12 hours at 490°C in 0.1~1.0% O_2 in N_2 gives severe oxidative decomposition without oxygen

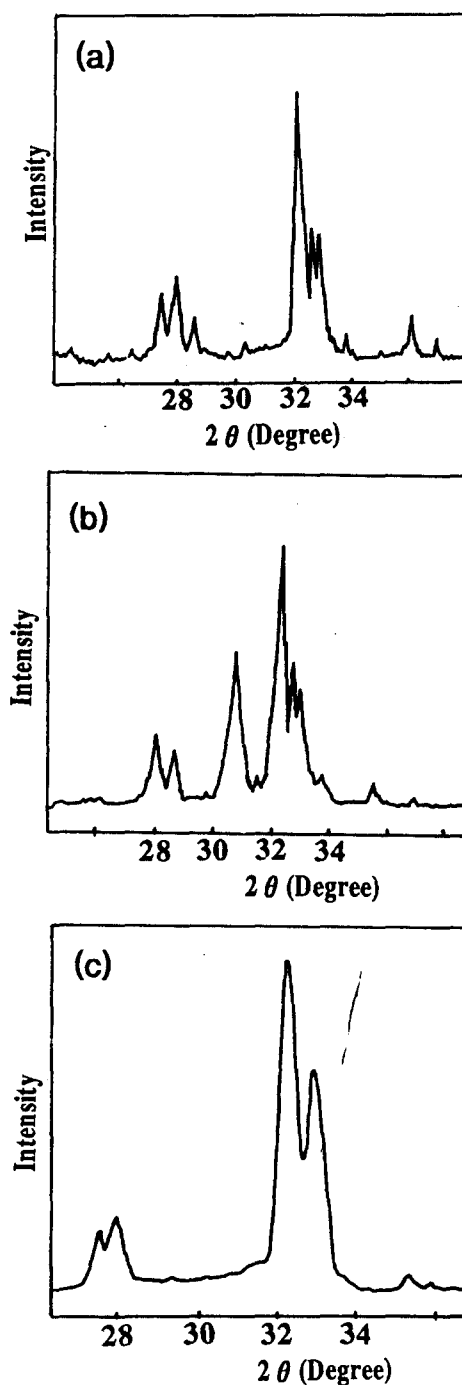


Fig. 3. XRD spectra for $\text{Pb}_2\text{Sr}_2(\text{Y}_{0.5}\text{Ca}_{0.5})\text{Cu}_3\text{O}_{8+\delta}$ after (a) sintering in 100% Ar ($\delta=0.0$), (b) annealed for 12 hours at 490 in 0.1% O_2 in N_2 for sample (a), and (c) annealed for 12 hours at 490 in 100% O_2 for sample (a).

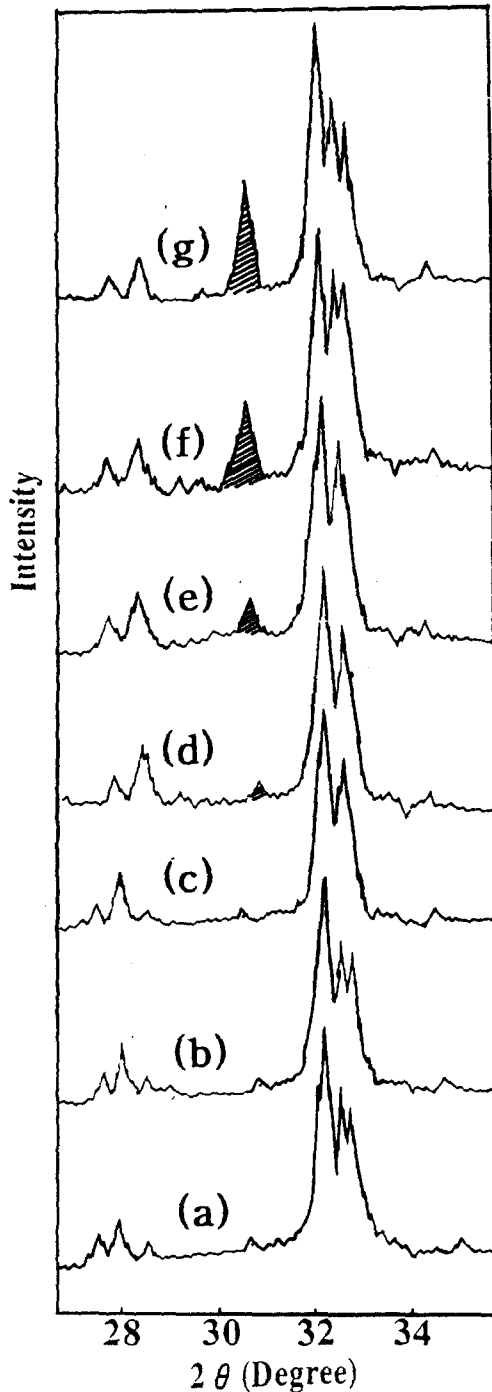


Fig. 4. XRD spectra for $\text{Pb}_2\text{Sr}_2(\text{Y}_{0.4}\text{Ca}_{0.6})\text{Cu}_3\text{O}_{8+\delta}$: (a) after the reaction for 1 hour ($\delta=0$), (b) after the sintering for 1 hour ($\delta=0$), (c) after the oxygenation for 4 hours ($\delta=1.83$), (d) after the deoxygenation for 2 hours under 0.1% O_2 in N_2 ($\delta=1.45$). Results obtained after the deoxygenation for 5 ($\delta=0.98$), 9 ($\delta=0.79$) and 12 ($\delta=0.82$) hours under 0.1% O_2 in N_2 are shown in (e), (f) and (g), respectively. Shaded peaks refer to the oxidative decomposition product.

intercalation (See Fig. 3b) although it decreases as lower the temperature to 470°C. However, annealing for 12 hours at 490°C in air or 100% O_2 shows a fully intercalated structure, with no sign of oxidative decomposition as shown in Fig. 3c. This surprising result implies that as oxygen is introduced into the structure, it becomes more stable against oxidative decomposition, or that the kinetics of oxygen incorporation can be made to dominate. Therefore, one last strategy for tuning the oxygen content of the high Ca materials is to react and sinter in Ar atmosphere, and then rapidly oxidize at $\sim 490^\circ\text{C}$ in 100% O_2 to form the tetragonal structure, followed by reduction in low oxygen partial pressures to the optimum oxygen content. This strategy hereafter was used to synthesize our samples.

Fig. 4 shows the powder x-ray diffraction pattern obtained for $\text{Pb}_2\text{Sr}_2(\text{Y}_{0.4}\text{Ca}_{0.6})\text{Cu}_3\text{O}_{8+\delta}$ (i.e., $x=0.6$) under various conditions. The two split peaks at $2\theta=33.3^\circ$ and 33.8° in Figs. 4a, b, f and g represent that the phases are orthorhombic while the phases shown in Figs. 4c-e are tetragonal. According to the δ value of each phase, it is clear that the sample is orthorhombic when $\delta < \sim 1.0$, but tetragonal otherwise. Figs. 4a-g show a key portion of the XRD patterns for samples prepared using different calcining and sintering times. Once oxygen is fully intercalated [see Fig. 4c] into the Cu(2) plane, minimal oxidative decomposition occurs during the first 5 hours of deoxygenation [see Figs. 4d and e]. But further oxygen removal, which is necessary to obtain a smaller δ value to be a superconductor, cause extensive oxidative decomposition, as shown in Figs. 4f and g.

Figs. 5. and 6 show the XRD patterns for the phases $\text{Pb}_2\text{Sr}_2(\text{Y}_{1-x}\text{Ca}_x)\text{Cu}_3\text{O}_{8+\delta}$ with $x=0.4$ and 0.5, respectively. The trends of these results are quite similar to those shown in Fig. 4. However, a lower oxygen content (i.e., smaller δ) can be achieved more easily as the calcium content in the samples is lowered (i.e.,

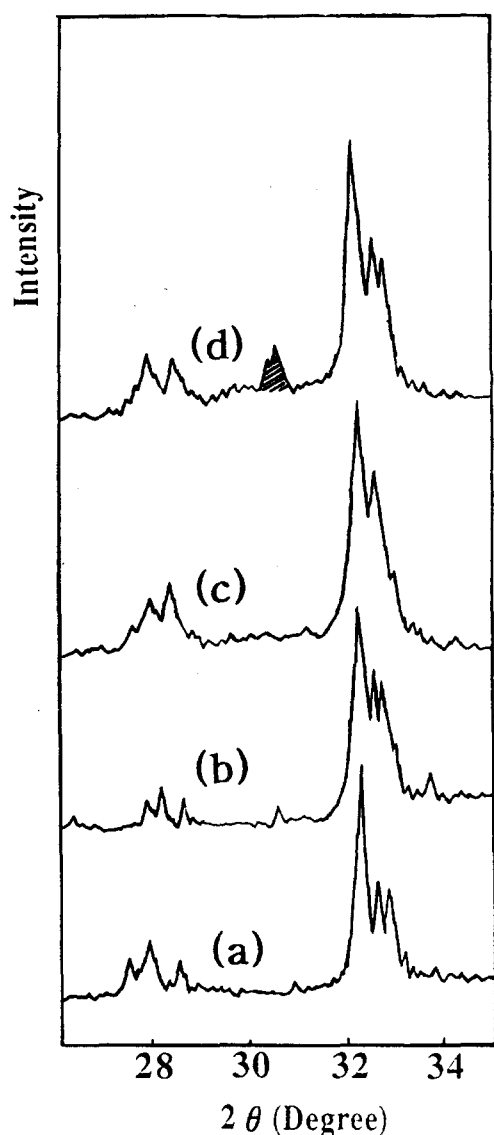


Fig. 5. XRD spectra for $\text{Pb}_2\text{Sr}_2(\text{Y}_{0.6}\text{Ca}_{0.4})\text{Cu}_3\text{O}_{8+\delta}$: (a) after the reaction for 1 hour ($\delta=0$), (b) after the sintering for 1 hour ($\delta=0$), (c) after the oxygenation for 1.5 hours ($\delta=1.33$), and (d) after the deoxygenation for 11 hours under 0.1% O_2 in N_2 ($\delta=0.59$). Shaded peaks refer to the oxidative decomposition product.

$\delta=0.59, 0.70$ and 0.98 when $x=0.4, 0.5$ and 0.6 , respectively, with a similar extent of oxidative decomposition). A slight change in the oxygen partial pressure in the deoxygenation step (e.g., 0.1 vs. 0.5% O_2 in N_2) does not affect

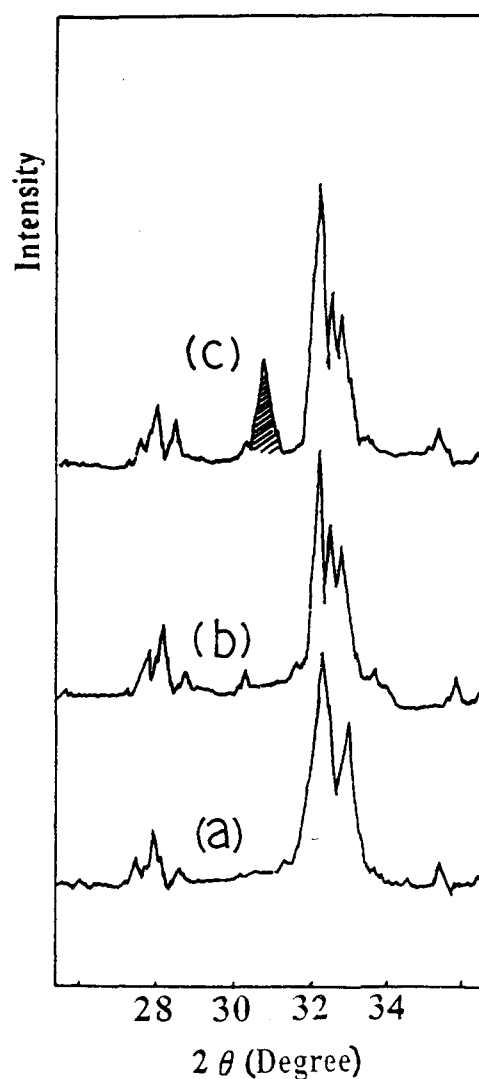


Fig. 6. XRD spectra for $\text{Pb}_2\text{Sr}_2(\text{Y}_{0.5}\text{Ca}_{0.5})\text{Cu}_3\text{O}_{8+\delta}$: (a) after the oxygenation for 1.5 hours ($\delta=1.60$), (b) after the deoxygenation for 2 hours under 0.5% O_2 in N_2 ($\delta=1.28$), and (c) after the deoxygenation for 4 hours under 0.5% O_2 in N_2 ($\delta=0.70$). Shaded peaks refer to the oxidative decomposition product.

the oxidative decomposition significantly. Details of our experimental results are summarized in Table 1. It is clear from Table 1 that controlling the oxygen content in the desired range without significant oxidative decomposition becomes more difficult as x is increased.

Table 1. Summary of the Phase Study Data

Reaction	Process Conditions			Composition*	2213 phase	Decomposition
	Sintering	O ₂ Anneal	LowPo ₂ Anneal			
800°C/Ar (1 hr.)				Ca 0.6 Ca 0.4	Ortho Ortho	Nil Nil
800°C/Ar (1 hr.)	800°C/Ar (1 hr.)			Ca 0.6 Ca 0.5 Ca 0.4	Ortho Ortho Ortho	Nil Nil Nil
800°C/Ar (1 hr.)	800°C/Ar (4 hrs.)			Ca 0.6 Ca 0.5	Ortho † Ortho †	Very slight Very slight
800°C/Ar (1 hr.)	800°C/Ar (1 hr.)	480°C/100% O ₂ (1.5 hrs.)		Ca 0.6 Ca 0.4	Tetrag Tetrag	Very slight Very slight
800°C/Ar (1 hr.)	800°C/Ar (1 hr.)	480°C/100% O ₂ (4 hrs.)		Ca 0.6	Tetrag	Very slight
800°C/Ar (1 hr.)	800°C/Ar (4 hrs.)	480°C/100% O ₂ (7 hrs.)		Ca 0.6 Ca 0.5	Tetrag Tetrag	Very slight Very slight
800°C/Ar (1 hr.)	800°C/Ar (1 hr.)	480°C/100% O ₂ (1.5 hrs.)	480°C/D.5% O ₂ (2 hrs.)	Ca 0.6	Tetrag	Decomposition
800°C/Ar (1 hr.)	800°C/Ar (1 hr.)	480°C/100% O ₂ (1.5 hrs.)	480°C/1.0% O ₂ (4 hrs.)	Ca 0.6	Tetrag	Decomposition
800°C/Ar (1 hr.)	800°C/Ar (1 hr.)	480°C/100% O ₂ (7 hrs.)	480°C/1.0% O ₂ (7 hrs.)	Ca 0.6 Ca 0.5	Tetrag Ortho (+ tetrag)	Large Slight
800°C/Ar (1 hr.)	800°C/Ar (1 hr.)	480°C/100% O ₂ (1.5 hrs.)	480°C/0.1% O ₂ (10.8 hrs.)	Ca 0.4	Ortho (+ sm. tetrag)	Slight
800°C/Ar (1 hr.)	800°C/Ar (1 hr.)	480°C/100% O ₂ (4 hrs.)	480°C/0.1% O ₂ (2 hrs.)	Ca 0.6	Tetrag	Very slight
800°C/Ar (1 hr.)	800°C/Ar (1 hr.)	480°C/100% O ₂ (4 hrs.)	480°C/0.1% O ₂ (5 hrs.)	Ca 0.6	Tetrag	Slight
800°C/Ar (1 hr.)	800°C/Ar (1 hr.)	480°C/100% O ₂ (4 hrs.)	480°C/0.1% O ₂ (9 hrs.)	Ca 0.6	Tetrag (+ ortho)	Large
800°C/Ar (1 hr.)	800°C/Ar (1 hr.)	480°C/100% O ₂ (4 hrs.)	480°C/0.1% O ₂ (12 hrs.)	Ca 0.6	Tetrag (+ ortho)	Large
800°C/Ar (1 hr.)	800°C/Ar (1 hr.)	480°C/100% O ₂ (4 hrs.)	480°C/10.5% O ₂ (13 hrs.)	Ca 0.6	Tetrag (+ ortho)	Large

* in $\text{Pb}_2\text{Sr}_2(\text{Ca}, \text{Y}_{1-x})\text{Cu}_3\text{O}_{8+\delta}$

† Poorly crystalline

Figs 7a and b show typical electrical resistance vs. temperature data obtained for the samples with $x=0.4$ and 0.5 after the sintering steps (i.e., $\delta \cong 0$), respectively. The transitions are broad with $T_c(\text{onset})=80\text{K}$. Although not shown, similar results are obtained for the samples with $x=0.6$. After the oxygenation step (i.e., δ is large), the

resistance increases by several orders of magnitude, and semiconducting behavior is observed [see Fig. 7c]. The deoxygenation step improves the electrical properties of the sample to where $T_c(\text{onset}) \sim 80\text{K}$ and $T_c(\text{zero}) \sim 45\text{K}$, as shown in Fig. 7d for the sample with $x=0.6$. However, the transition is still broad, and this might be attributed to decom-

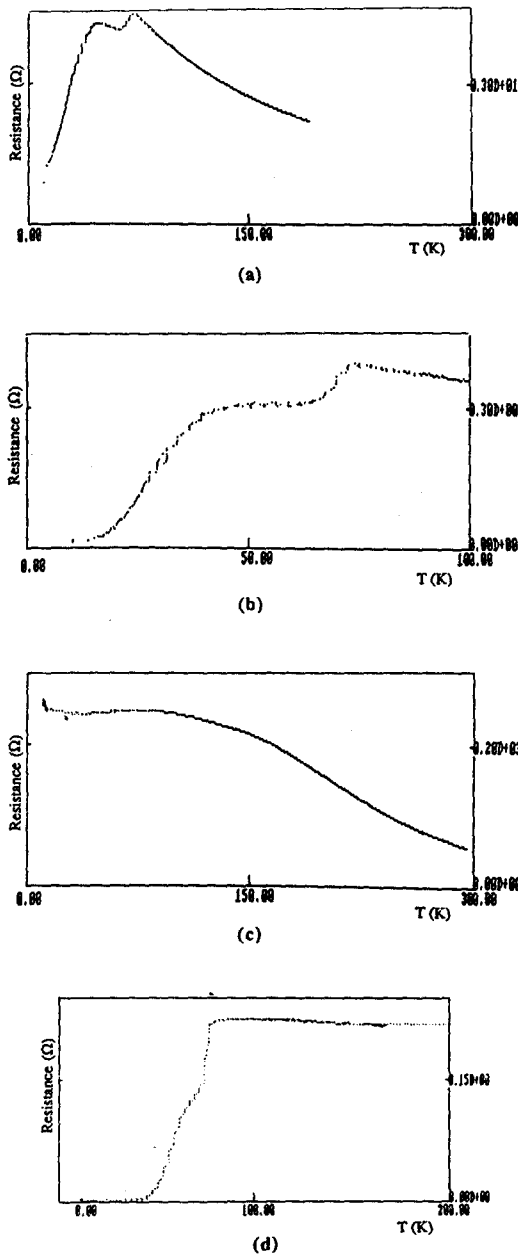


Fig. 7. Temperature vs electrical resistance plot for $\text{Pb}_2\text{Sr}_2(\text{Y}_{0.5}\text{Ca}_{0.5})\text{Cu}_3\text{O}_{8+\delta}$ (a) after the sintering with a sample of $x=0.4$, (b) after the sintering with a sample of $x=0.5$, (c) after the oxygenation for 1 hour with a sample of $x=0.4$, and (d) after the deoxygenation for 9 hours with a sample of $x=0.6$.

position products formed during the deoxygenation step. The samples with longer deoxygenation time (more than 9 hours) show

broader transitions, which is consistent with the XRD data that the oxidative decomposition becomes more competitive as the deoxygenation time increases. Resistivity measurements show that the $T_c(\text{onset}) \sim 80\text{K}$ when $x=0.5$ and 0.6. This implies that the optimum hole concentration in the CuO_2 layer can be achieved when Ca^{2+} substitution for Y^{3+} is 50~60 mole%. Trends in $T_c(\text{onset})$ vs hole concentration are consistent with earlier work. It is quite difficult to optimize the processing conditions to synthesize the homogeneous 2213-phase.

IV. Conclusions

$\text{Pb}_2\text{Sr}_2(\text{Y}_{1-x}\text{Ca}_x)\text{Cu}_3\text{O}_{8+\delta}$ samples were prepared with $x=0.4\sim 0.6$ and small δ . To minimize the extent of oxidative decomposition reaction which occurs during the preparation of this phase, two annealing steps were adopted: First, sintered samples of $\text{Pb}_2\text{Sr}_2(\text{Y}_{1-x}\text{Ca}_x)\text{Cu}_3\text{O}_{8+\delta}$ are oxygenated under 100% O_2 , which leads to a large δ (e.g., $\delta=1.8$). Second, the resulting samples are deoxygenated under 0.1~1.0% O_2 in N_2 , lowering δ to desired values. This two-step annealing procedure minimized the extent of oxidative decomposition. However, even with the two-step annealing procedure, the oxidative decomposition of $\text{Pb}_2\text{Sr}_2(\text{Y}_{1-x}\text{Ca}_x)\text{Cu}_3\text{O}_{8+\delta}$ cannot be completely suppressed if δ is to be reduced to maximize T_c .

Electrical resistivity data show that $T_c(\text{onset})$ is a function of hole concentration in the CuO_2 layer, and the optimum hole concentration for the maximum T_c is achieved when Ca^{2+} is substituted for Y^{3+} between 0.5 and 0.6. A $T_c(\text{onset})=80\text{K}$ has been observed for one such sample, and this is the highest $T_c(\text{onset})$ yet reported for this compound.

Because the kinetics of high-temperature bulk processing favor oxidative decomposition over increased hole doping, any further improvements in properties for this compound might arise from non-equilibrium processing. Unless further improvements can be found, the difficult synthesis and limited properties of the

2213-phase preclude its applicability in nitrogen-cooled superconductor technologies.

Acknowledgements

The authors thank Wonkwang University for the financial support during this research.

V. References

1. R. J. Cava, B. Batlogg, J. J. Krajewski, L. W. Rupp, L. F. Schneemeyer, T. Siegrist, R. B. van Dover, P. Marsh, W. F. Peck Jr., P. K. Gallapther, S.H. Glarum, J.H. Glarum, J. H. Marshall, R.C. Farrow, J. V. Waszczak, R. Hull, and P. Trevor, *Nature* 336, 211 (1988)
2. (a) Z.Z. Sheng and A.M. Hermann, *Nature* 332, 138(1988)
(b) H. Maeda, Y. Tanaka, M. Fukutomi, and T. Asano, *Jpn. J. Appl. Phys.* 27, L209(1988)
3. (a) J.M. Longo and P.M. Raccach, *J. Solid State Chem.*, 6, 526(1973).
(b) M.-H. Whangbo, M. Evain, M.A. Beno, and J.M. Williams, *Inorg. Chem.*, 29, 1829(1987).
4. M.A. Subramanian, J. Gopalakrishnan, C.C. Torardi, P.L. Gai, E.D. Boyes, T.R. Askew, R.B. Flippen, W.E. Farneth, and A.W. Sleight, *Physica C* 157, 124(1989).
5. H.W. Zandbergen, W.T. Fu, K. Kadowaki, and G. van Tendeloo, *Physica C* 161, 390 (1989).
6. (a) M.W. Shafer, T. Penney, and B.L. Olson, *Phys. Rev.*, B36, 4047(1988).
(b) M.-H. Whangbo, D.B. Kang, and C.C. Torardi, *Physica C* 160, 381(1989).
7. (a) P.K. Gallapther, H.M. O'Bryan, R.J. Cava, A.C.P.W. James, D.W. Murphy, W.W. Rhodes, J.J. Krajewski, W.F. Peck Jr., and J.V. Waszczak, *Chem. Mat.* 1, 277(1989).
(b) H.W. Zandbergen, K. Kadowaki, M.J. V. Menken, A.A. Menovsky, G. van Tendeloo, and S. Amelinckx, *Physica C* 158, 155(1989).
(c) L.F. Schneemeyer, R.J. Cava, A.C.P. W. James, P. Marsh, T. Siegrist, J.V. Waszczak, J.J. Krajewski, W.F. Peck Jr., R.L. Opila, S.H. Glarum, J.H. Marshall, R. Hull, and J.M. Bonar, *Chem. Mat.*, 1, 548(1989).